Wnt Antagonist SFRP1 Functions as a Secreted Mediator of Senescence

David J. Elzi,[a] Meihua Song,[a] Kevin Hakala,[b] Susan T. Weintraub,[b,c] and Yuzuru Shiio[a,b,c]

Greehey Children's Cancer Research Institute,[a] Department of Biochemistry,[b] and Cancer Therapy and Research Center,[c] The University of Texas Health Science Center, San Antonio, Texas, USA

Cellular senescence has emerged as a critical tumor suppressive mechanism in recent years, but relatively little is known about how senescence occurs. Here, we report that secreted Frizzled-related protein 1 (SFRP1), a secreted antagonist of Wnt signaling, is oversecreted upon cellular senescence caused by DNA damage or oxidative stress. SFRP1 is necessary for stress-induced senescence caused by these factors and is sufficient for the induction of senescence phenotypes. We present evidence suggesting that SFRP1 functions as a secreted mediator of senescence through inhibition of Wnt signaling and activation of the retinoblastoma (Rb) pathway and that cancer-associated SFRP1 mutants are defective for senescence induction.

After a limited number of cell divisions, primary cells in culture undergo an irreversible proliferation arrest called replicative senescence (17). Different stresses such as DNA damage or oncogene expression can also induce similar, persistent proliferation arrest, which is called stress-induced senescence (6, 22). Accumulating evidence suggests that cellular senescence plays important roles in organismal aging and tumor suppression (6, 22), but the signaling pathways mediating senescence are only incompletely understood.

In addition to persistent proliferation arrest, senescent cells often display characteristic phenotypes such as flat and enlarged morphology, senescence-associated beta-galactosidase (SA-β-Gal) activity (13), senescence-associated heterochromatic foci (SAHF) (28), and increased expression of cell cycle inhibitors (6, 22). Further, a number of studies identified altered protein secretion from senescent cells, which is collectively called the senescence-associated secretory phenotype (SASP) (10) or senescence-messaging secretome (SMS) (24). These include increased secretion of inflammatory cytokines such as interleukins and chemokines, proteases, and regulators of insulin-like growth factor (IGF) signaling. These SASP or SMS factors may recruit immune cells for clearance of senescent cells, affect the architecture or function of surrounding tissues, modulate tumor progression, and contribute to aging and age-related diseases.

We undertook a quantitative proteomic analysis of proteins secreted from human primary fibroblasts induced to senesce by DNA damage, Ras oncogene, or replicative telomere shortening and identified the oversecretion of a number of SASP/SMS factors. This analysis also identified the oversecretion of secreted Frizzled-related protein 1 (SFRP1), a secreted antagonist of Wnt signaling, upon DNA damage-induced senescence. SFRP1 oversecretion occurred upon treatment with different DNA damaging agents or in response to oxidative stress and was required for stress-induced senescence. We present evidence suggesting that secreted SFRP1 mediates senescence by inhibiting the Wnt signaling pathway and activating the retinoblastoma (Rb) pathway and that SFRP1 mutations found in human cancers impair the senescence-inducing activity of SFRP1.

MATERIALS AND METHODS

Reagents. Recombinant SFRP1 was from R&D Systems. Etoposide was from Calbiochem/EMD Biosciences. Caffeine, doxorubicin, hydrogen peroxide, brefeldin A, heparin, Hoechst 33258, bromodeoxyuridine (BrdU), and pyrvinium pamoate were from Sigma-Aldrich. Hygromycin and trypan blue were from Invitrogen. Lithium chloride was from Acros Organics. cDNAs for SFRP1, SFRP3, and SFRP4 were from the Dana Faber/Harvard Cancer Center DNA resource core. cDNAs for SFRP2, SFRP5, and Wnt3 were from Open Biosystems. DKK1 cDNA was a gift of Sergei Sokol (Addgene plasmid 15494). Human Bik cDNA was cloned by reverse transcription-PCR (RT-PCR). pCDF1-MCS2-EF1-Puro (for cDNA expression) and pSIF1-H1-Puro (for short hairpin RNA [shRNA] expression) lentiviral vectors were from System Biosciences. The target sequences for shRNAs are as follows: human SFRP1 shRNA-1, AGAAGA AGGACCTGAAGAA; SFRP1 shRNA-3, TGAAGAAGCTTGTGCTGTA; luciferase shRNA, GCACTCTGATTGACAAATACGATTT; β-catenin shRNA-1, AGGTGCTATCTGTCTGCTCTA; β-catenin shRNA-2, GCTT GGAATGAGACTGCTGATCT; scrambled shRNA, CCTAAGGTTAAGT CGCCCTCGCT; Rb shRNA-1, GGTTGTGTCGAAATTGGATCA; Rb shRNA-2, CAGAGATCGTGTATTGAGATT; p53 shRNA-1, GACTCCA GTGGTAATCTACT; and p53 shRNA-2, GAAATTTGCGTGTGGAGTA.

Cell culture. IMR-90 and MRC-5 fibroblasts (purchased from ATCC) and RPE-28 cells (purchased from Coriell Institute) were cultured in Dulbecco's modified Eagle's medium (DMEM) supplemented with 10% fetal calf serum. 293 and 293T cells were cultured in DMEM supplemented with 10% calf serum. Human mammary epithelial cells and their culture medium were purchased from Lonza. MCF-7 cells were cultured in minimum essential medium supplemented with 10% fetal calf serum and nonessential amino acids. Lipofectamine 2000 reagent (Invitrogen) was used for transfection of IMR-90 cells. Calcium phosphate coprecipitation was used for transfection of other cell types. Lentiviruses were prepared by transfection in 293T cells following the protocol of System Biosciences. The cells infected with lentiviruses were selected with 2 μg/ml puromycin for 48 h. For coinfection experiments, the infected cells were selected with 2 μg/ml puromycin and 0.15 mg/ml hygromycin for 48 h.

Senescence-associated beta-galactosidase assays (13) and detection of senescence-associated heterochromatic foci (SAHF) (28) were conducted

as described previously. A minimum of 100 cells were counted. For antibody blocking experiments, cells were treated with 1 µg/ml of neutralizing antibodies or IgG 24 h after etoposide treatment or SFRP1 viral infection. In selected experiments, antibodies were incubated with an equal amount of blocking peptide or immunogen for 30 min before being added to the cells. For coculture experiments, young IMR-90 cells were green fluorescent protein (GFP) labeled by infection with GFP-expressing lentivirus. These cells were cocultured with etoposide-treated IMR-90 cells (20 µM for 2 days), SFRP1-expressing IMR-90 cells, or control cells for 4 days. The GFP-positive cells were scored for SAHF.

Protein sample preparation, ICAT reagent labeling, and mass spectrometry. To induce senescence, (i) IMR-90 cells were treated with 20 µM etoposide for 48 h and then cultured without etoposide for 6 days; (ii) IMR-90 cells were infected with c-H-RasV12-expressing lentivirus (empty vector lentivirus as a control), selected with 2 µg/ml puromycin for 48 h, and cultured until 8 days postinfection; or (iii) IMR-90 cells were cultured until they senesced by replicative telomere shortening. Senescent and control nonsenescent IMR-90 fibroblasts were washed six times with phosphate-buffered saline (PBS), and the medium was changed to DMEM without serum. The cells were cultured for another 24 h, and the culture supernatant was harvested. The supernatant was centrifuged, filtered through a 0.45-µm-pore-size filter (Millipore), and concentrated using a 3,000-Da-cutoff Centriprep spin column (Millipore). The sample was further concentrated using a 3,000-Da-cutoff Microcon spin column (Amicon). A 100-µg protein sample (for replicative senescence and Ras-induced senescence) or 200-µg protein sample (for etoposide-induced senescence) was used for isotope-coded affinity tag (ICAT) reagent labeling (senescent cell sample, isotopically light ICAT reagent; control nonsenescent cell sample, isotopically heavy ICAT reagent). The two labeled samples (senescent and nonsenescent) were combined, digested with trypsin, and fractionated by cation exchange chromatography. ICAT reagent-labeled peptides were purified using the biotin tag present in the reagent and analyzed by microcapillary high-performance liquid chromatography-tandem mass spectrometry (µLC-MS/MS) using a Thermo Fisher linear trap quadrupole (LTQ) mass spectrometer as described previously (16, 25, 36). Tandem mass spectra were searched against the human International Protein Index (IPI) protein database using the SEQUEST algorithm (14). Peptide/protein identification was validated by Peptide/ProteinProphet software tools (21, 30). A ProteinProphet score of 0.5 was used as a cutoff. Protein abundance ratios were calculated using the ASAPRatio software tool (26).

Immunoblotting, immunofluorescence, and antibodies. Unless otherwise noted in the figure legends, 30 µg of whole-cell lysate or 10 µg of conditioned medium was separated by SDS-PAGE and analyzed by immunoblotting as described previously (36). Soluble β-catenin protein levels were determined as described previously (42) using 5 µg of soluble fractions. Immunofluorescence was performed as described previously (36). The following antibodies were used: rabbit polyclonal anti-SFRP1 (H-90; Santa Cruz Biotechnology), goat polyclonal anti-SFRP1 (C-19; Santa Cruz Biotechnology), rabbit monoclonal anti-SFRP1 (D5A7, used for immunoblotting; Cell Signaling), rabbit polyclonal anti-SPARC (H-90; Santa Cruz Biotechnology), mouse monoclonal antinucleolin (C23; Santa Cruz Biotechnology), rabbit polyclonal anti-β-catenin (GenScript), mouse monoclonal anti-Rb (G3-245; BD Pharmingen), rabbit polyclonal anti-p53 (FL-393; Santa Cruz Biotechnology), mouse monoclonal anti-p21 (SX118; BD Pharmingen), mouse monoclonal anti-LAMP2 (555803; BD Pharmingen), rabbit monoclonal anti-mammalian target of rapamycin (anti-mTOR) (7C10; Cell Signaling), mouse monoclonal anti-FLAG (M2; Sigma-Aldrich), mouse monoclonal antitubulin (DM1A; Sigma-Aldrich), mouse monoclonal anti-BrdU (BD Pharmingen), rabbit polyclonal anti-Ki-67 (Abcam), rabbit polyclonal anti-trimethylated lysine-9 histone H3 (ab8898; Abcam), rabbit polyclonal antiactin (ab1801; Abcam), rabbit monoclonal anti-caspase 3 (8G10; Cell Signaling), rabbit polyclonal anti-poly(ADP-ribose) polymerase (anti-PARP) (9542; Cell Signaling), and

goat polyclonal anti-phosphoglycerate kinase 1 (anti-PGK1) (sc-17943; Santa Cruz Biotechnology).

RT-PCR. Total cellular RNA was prepared using TRIzol reagent (Invitrogen), and RT-PCR was performed as described previously (37). The following PCR primers were used: RNA polymerase II (Pol II) 5′ primer, GGATGACCTGACTCACAAACTG, and 3′ primer, CGCCCAGACTTC TGCATGG; SFRP1 5′ primer, AACGTGGGCTACAAGAAGATG, and 3′ primer, CAGCGACACGGGTAGATGG; CXCL1 5′ primer, CTTCCTCC TCCCTTCTGGTC, and 3′ primer, GAAAGCTTGCCTCAATCCTG; interleukin 1α (IL-1α) 5′ primer, CCGTGAGTTTCCCAGAAGAA, and 3′ primer, ACTGCCCAAGATGAAGACCA; IL-8 5′ primer, AAATTTGGG GTGGAAAGGTT, and 3′ primer, TCCTGATTTCTGCAGCTCTGT; c-myc 5′ primer, GCTGCTTAGACGCTGGATTT, and 3′ primer, CTCCT CCTCGTCGCAGTAGA; CDC25A 5′ primer, TAAGACCTGTATCTCG TGGCTG, and 3′ primer, CCCTGGTTCACTGCTATCTCT; and cyclin D1 5′ primer, GAACAAACAGATCATCCGCAAAC, and 3′ primer, GC GGTAGTAGGACAGGAAGTTG.

Luciferase reporter assay. Super TopFlash reporter was described previously (43). A luciferase assay was performed as described previously (37).

Statistical analysis. WINKS statistical analysis software (Texasoft, Cedar Hill, TX) was used. Data are expressed as the means ± standard deviations. Statistical significance was determined by analysis of variance (ANOVA) and a *post hoc* Newman-Keuls analysis. A P value of <0.05 was considered significant.

RESULTS

Quantitative proteomics identifies SFRP1 oversecretion upon DNA damage-induced senescence. We employed a quantitative proteomics approach to identify the protein secretion changes associated with cellular senescence that is induced by different stimuli. Human IMR-90 fibroblasts were induced to senesce by etoposide, oncogenic Ras (c-H-RasV12), or replicative telomere exhaustion, and the proteins secreted in the conditioned medium were identified and quantified (in comparison with nonsenescent IMR-90 cells) by isotope-coded affinity tag (ICAT) technology (16, 35). The complete lists of proteins identified and quantified in the three secretome analyses are shown in Table S1 in the supplemental material. We determined that a number of previously reported SASP/SMS factors are oversecreted in different combinations from three types of senescent cells. In addition, we also identified novel protein secretion changes such as oversecretion of SFRP1 upon etoposide-induced senescence.

SFRP1 is a secreted antagonist of Wnt signaling and functions as a tumor suppressor (4, 15, 20). We verified the increased secretion of SFRP1 upon etoposide treatment of IMR-90 fibroblasts and a second human primary fibroblast line, MRC-5, by immunoblotting of the secreted protein samples (Fig. 1A). Whereas SFRP1 mRNA expression did not change upon etoposide treatment (Fig. 1B), SFRP1 protein abundance in the whole-cell lysate of IMR-90 cells treated with brefeldin A, an inhibitor of protein transport from endoplasmic reticulum (ER) to the Golgi compartment, displayed pronounced increase upon etoposide treatment (Fig. 1C). This suggests that SFRP1 oversecretion upon etoposide treatment is due to enhanced SFRP1 protein entry to the secretory pathway. Increased intracellular SFRP1 upon etoposide treatment was not observed in the absence of brefeldin A, which suggests that SFRP1 entering the secretory pathway is quickly secreted. A previous study demonstrated that a significant fraction of secreted SFRP1 is attached to the cell surface and can be efficiently released to the culture medium by heparin treatment (15). We found that heparin increases the levels of free extracellular
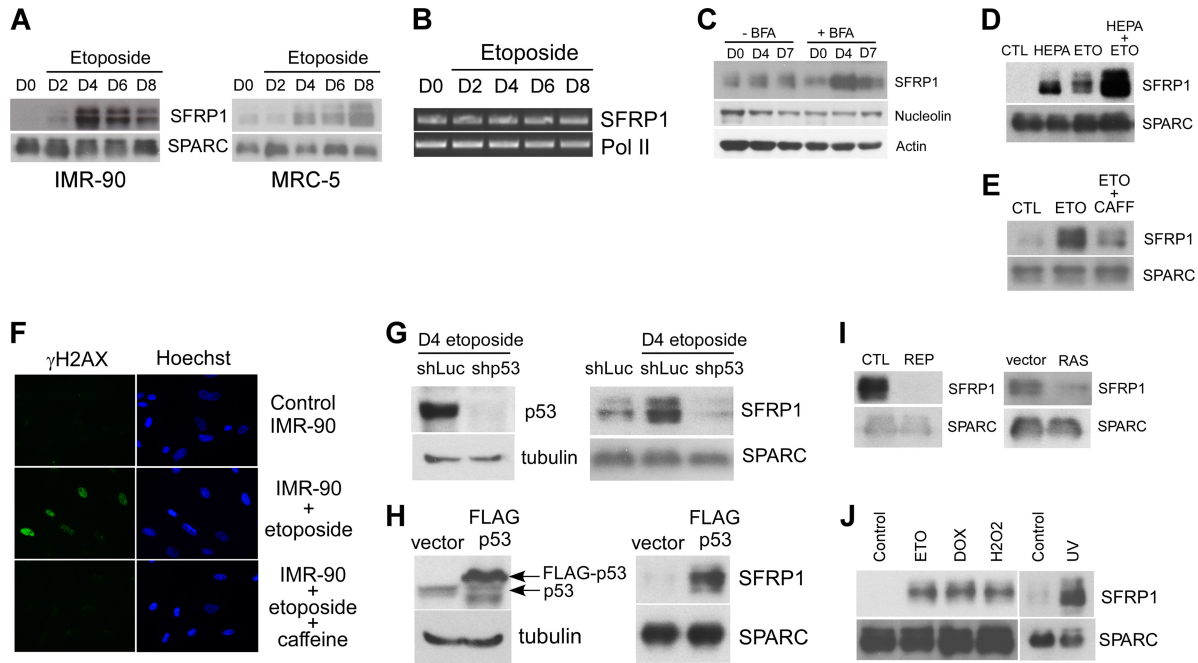
FIG 1 Stress-induced SFRP1 secretion. (A) Secretion of SFRP1 from etoposide-treated IMR-90 and MRC-5 cells. IMR-90 and MRC-5 cells were treated with 20 µM etoposide for 48 h. On the indicated days after initiating the etoposide treatment, conditioned medium was collected and concentrated. Conditioned medium from untreated cells (day 0 [D0]) was also included as a control. Ten micrograms of each conditioned medium was analyzed for SFRP1 levels by immunoblotting. SPARC (secreted protein, acidic, cysteine rich) served as a loading control. (B) RNA levels of SFRP1 after etoposide treatment of IMR-90 cells. IMR-90 cells were treated with 20 µM etoposide for 48 h. At the indicated time points after initiating the etoposide treatment, total RNA was isolated. Total RNA from untreated cells (D0) was also included as control. RT-PCR analysis was performed for mRNA levels of SFRP1 and RNA polymerase II (Pol II, loading control). (C) Increased SFRP1 entry to the secretory pathway upon etoposide treatment. IMR-90 cells were left untreated (D0) or treated with 20 µM etoposide for 48 h. At the indicated time points after initiating the etoposide treatment, whole-cell lysates were prepared with or without brefeldin A (BFA) treatment (5 µg/ml for 2 h) and were analyzed for SFRP1 levels by immunoblotting. Nucleolin and actin served as loading controls. (D) Etoposide (ETO) increases extracellular SFRP1 levels in the presence of heparin (HEPA). IMR-90 cells were treated with 50 µg/ml heparin or 20 µM etoposide or both for 48 h. Four days after each treatment was initiated, the SFRP1 protein present in the conditioned medium was determined by anti-SFRP1 immunoblotting. (E and F) Inhibition of SFRP1 secretion by caffeine. IMR-90 cells were left untreated, treated with 20 µM etoposide for 48 h, or treated with 5 mM caffeine (CAFF) overnight prior to treatment with 20 µM etoposide for 48 h. Four days after etoposide treatment, the secretion of SFRP1 and SPARC was analyzed by immunoblotting (E), and the DNA damage response was assessed by γH2AX staining (F). (G) Etoposide-induced SFRP1 secretion is p53 dependent. IMR-90 cells were infected with lentiviruses expressing shRNA against luciferase (shLuc, control) or shRNA against p53 (shp53) and were selected with 2 µg/ml puromycin. The selected cells were treated with 20 µM etoposide for 48 h. Five days after the etoposide treatment was initiated, conditioned medium was collected and was analyzed for SFRP1 and SPARC levels by immunoblotting (right). p53 knockdown was verified by anti-p53 immunoblotting of the whole-cell lysates (left). (H) p53 induces SFRP1 secretion. IMR-90 cells were infected with empty vector or FLAG-p53-expressing lentivirus. Four days later, the expression of p53 and tubulin was analyzed by immunoblotting of the whole-cell lysates (left), and the secretion of SFRP1 and SPARC was analyzed by immunoblotting of the conditioned medium (right). (I) Secretion of SFRP1 from IMR-90 cells undergoing replicative senescence (REP) or Ras-induced senescence (RAS) was analyzed by anti-SFRP1 immunoblotting. CTL, control. (J) Different stresses induce SFRP1 secretion. IMR-90 cells were treated with 20 µM etoposide (ETO) for 48 h, 1 µM doxorubicin (DOX) for 2 h, 500 µM H_2O_2 for 2 h, or 2 J/m² UV light. Conditioned medium was collected at 4 days posttreatment and was analyzed for SFRP1 and SPARC levels by immunoblotting.

SFRP1 and that etoposide further increases the levels of free SFRP1 in the presence of heparin (Fig. 1D).

Caffeine-sensitive kinases such as ATM (ataxia-telangiectasia mutated) and ATR (ATM-Rad3-related) play pivotal roles in the DNA damage response. We found that caffeine blocks both DNA damage signaling and SFRP1 oversecretion upon etoposide treatment (Fig. 1E and F). ATM was recently shown to mediate senescence-associated inflammatory cytokine secretion (34). However, these inflammatory cytokines appear to be induced at transcriptional levels through NF-κB and C/EBPβ (1, 11, 23, 32), suggesting that the downstream pathway mediating posttranscriptional SFRP1 induction is distinct. We also found that p53 knockdown abrogates SFRP1 oversecretion upon etoposide treatment (Fig. 1G). Furthermore, lentiviral p53 expression in IMR-90 cells resulted in increased secretion of SFRP1 (Fig. 1H).

These results suggest that DNA damage enhances SFRP1 secretion by a p53-dependent mechanism. This is again in contrast to senescence-associated inflammatory cytokine secretion, which does not require p53 and is restrained by p53 (11).

A recent study suggested a role for a specialized cytoplasmic compartment, the TOR-autophagy spatial coupling compartment (TASCC), in protein secretion upon Ras-induced senescence (29). TASCC is detected as a discrete cytoplasmic blob-like structure where mTOR and LAMP2 colocalize (29). Whereas TASCC was readily detectable upon Ras-induced senescence of IMR-90 cells, we were not able to detect similar TASCC-like structures upon etoposide treatment or SFRP1 expression (Fig. 2A). Like endogenous SFRP1, lentivirally expressed, C-terminally FLAG-tagged SFRP1 displayed increased secretion upon etoposide-induced senescence (Fig. 2B). However, FLAG-tagged SFRP1 did not colo-
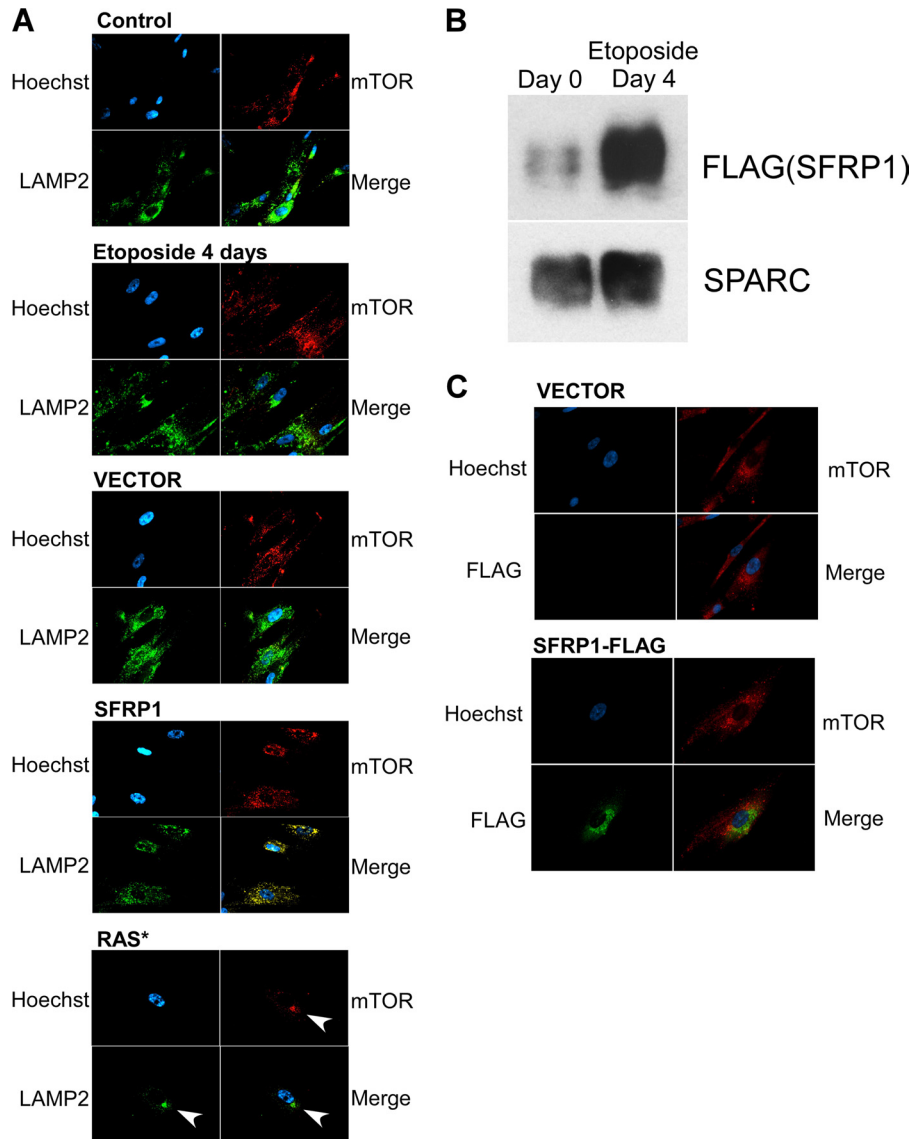
FIG 2 Lack of TASCC formation upon etoposide treatment or SFRP1 expression. (A) Subcellular location of mTOR and LAMP2 upon senescence induced by etoposide, SFRP1, or oncogenic Ras. The formation of TASCC (TOR-autophagy spatial coupling compartment) was assessed by staining for mTOR and LAMP2. Whereas TASCC was readily detectable upon Ras-induced senescence (arrows), TASCC formation was not observed upon etoposide-induced or SFRP1-induced senescence. (B) Etoposide increases the secretion of FLAG-tagged SFRP1. IMR-90 cells were infected with lentiviruses expressing C-terminally FLAG-tagged SFRP1 and were treated with etoposide. The levels of secreted FLAG-tagged SFRP1 were determined by anti-FLAG immunoblotting. (C) Lack of colocalization of FLAG-tagged SFRP1 and mTOR. IMR-90 cells were infected with lentiviruses expressing C-terminally FLAG-tagged SFRP1 or empty vector and were treated with etoposide. Four days later, the cells were stained for mTOR and FLAG.

calize with mTOR upon etoposide-induced senescence (Fig. 2C), unlike IL-8, which displayed colocalization with mTOR in TASCC upon Ras-induced senescence (29). These results suggest that TASCC is not involved in the oversecretion of SFRP1 upon etoposide-induced senescence.

While SFRP1 secretion did not increase upon Ras-induced or replication-induced senescence of IMR-90 cells (Fig. 1I; see also Table S1 in the supplemental material), cells undergoing stress-induced senescence (by etoposide, doxorubicin, UV, or hydrogen peroxide treatment) displayed enhanced SFRP1 secretion (Fig. 1J).

SFRP1 mediates senescence. Because SFRP1 expression is frequently silenced by promoter methylation in various types

of human cancers (4, 20, 38), we sought to determine whether SFRP1 mediates cellular senescence, which is widely considered a key tumor-suppressive mechanism. We first examined whether SFRP1 downregulation by RNA interference (RNAi) or by neutralizing antibody inhibits senescence induction. SFRP1 secretion from IMR-90 cells was efficiently suppressed by two different short hairpin RNAs (shRNAs) (Fig. 3A), which resulted in alleviation of etoposide-induced senescence (Fig. 3B and C). Furthermore, addition of anti-SFRP1 antibody to the culture medium also diminished etoposide-induced senescence of IMR-90 cells (Fig. 3D), suggesting a role for secreted extracellular SFRP1 in mediating etoposide-induced senescence. Anti-SFRP1 antibody did not have any effect on Ras-induced senescence of IMR-90 cells
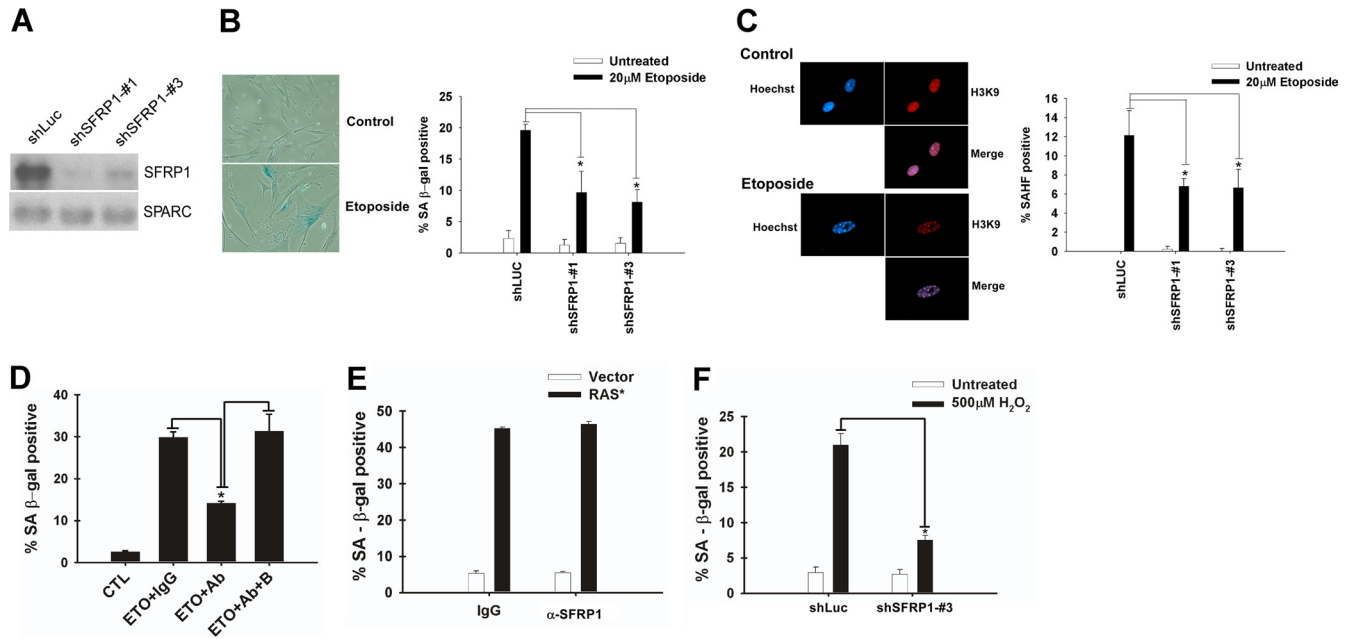
FIG 3 SFRP1 downregulation alleviates etoposide-induced senescence. (A) shRNA knockdown of SFRP1. IMR-90 cells were infected with lentiviruses expressing shRNA against luciferase (shLuc; control) or shRNAs against SFRP1 (shSFRP1-1 and shSFRP1-3) and were selected with 2 μg/ml puromycin. Five days after infection, conditioned medium was collected and was analyzed for SFRP1 and SPARC levels by immunoblotting. (B and C) SFRP1 knockdown attenuates etoposide-induced senescence. The effect of SFRP1 knockdown on etoposide-induced senescence of IMR-90 cells was analyzed 6 days after etoposide treatment. (B) SA-β-Gal staining. (C) Senescence-associated heterochromatic foci (SAHF). A minimum of 100 cells were counted. *, $P < 0.05$ compared to shLuc plus 20 μM etoposide. (D) SFRP1 antibody inhibits etoposide-induced senescence. IMR-90 cells were treated for 48 h with etoposide. Beginning 24 h after treatment, the cells were incubated with either 1 μg/ml of control rabbit IgG, anti-SFRP1 antibody (rabbit polyclonal H-90; Santa Cruz Biotechnology), or anti-SFRP1 antibody (Ab) plus immunogen (block [B]). Cells were assayed for SA-β-Gal staining 5 days after etoposide treatment. *, $P < 0.05$ compared to etoposide plus the IgG control or to etoposide plus anti-SFRP1 and block. (E) SFRP1 antibody does not affect Ras-induced senescence. IMR-90 cells were infected with c-H-RasV12-expressing lentivirus (empty vector lentivirus as a control). Beginning 4 days after infection, the cells were incubated with either 1 μg/ml of control rabbit IgG or anti-SFRP1 antibody. Eight days after infection, the cells were stained for SA-β-Gal. (F) SFRP1 knockdown abolishes oxidative stress-induced senescence. IMR-90 cells were treated with 500 μM H_2O_2 for 2 h. The following day, the cells were infected with lentiviruses expressing shRNA against luciferase or SFRP1. On day 6 after H_2O_2 treatment, the cells were analyzed for SA-β-Gal. *, $P < 0.05$.

(Fig. 3E). As mentioned above, SFRP1 is oversecreted upon different senescence-inducing stresses including hydrogen peroxide treatment. We found that SFRP1 knockdown efficiently inhibits hydrogen peroxide-induced senescence of IMR-90 cells (Fig. 3F), which suggests that SFRP1 also plays a role in oxidative stress-induced senescence.

We then tested whether SFRP1 upregulation induces senescence. Lentiviral SFRP1 expression in IMR-90 cells caused a striking proliferation arrest as determined by the lack of BrdU incorporation and Ki-67 staining (Fig. 4A and B), which was accompanied by senescence phenotypes including flat and enlarged morphology (Fig. 4C left), senescence-associated β-Gal activity (Fig. 4C), senescence-associated heterochromatic foci (Fig. 4D), and induction of genes representing a senescence-associated secretory phenotype (Fig. 4E). SFRP1 did not induce cell death or apoptosis in IMR-90 cells, whereas apoptosis induced by BH3-only protein Bik was readily detectable (Fig. 4F to H). Furthermore, addition of purified recombinant SFRP1 protein to the culture medium resulted in a senescence phenotype in IMR-90 cells (Fig. 4I). Consistent with the role of secreted SFRP1 in senescence induction, we also observed that nonsenescent IMR-90 cells acquire a senescence phenotype upon coculture with senescent IMR-90 cells which were induced to senesce by etoposide or by SFRP1 expression (Fig. 4J). This "spreading of senescence" was suppressed by the addition of anti-SFRP1 antibody to the culture medium (Fig. 4J).

The role of SFRP1 in cellular senescence was also examined in epithelial cells. Upon etoposide treatment, human primary retinal pigment epithelial cells (RPE-28) displayed SFRP1 oversecretion (Fig. 5A) and underwent senescence (Fig. 5B and C). Etoposide-induced senescence of RPE-28 cells was alleviated by SFRP1 shRNAs (Fig. 5B) or by the addition of anti-SFRP1 antibody to the culture medium (Fig. 5C). Furthermore, the addition of recombinant SFRP1 to the culture medium resulted in a senescence phenotype in RPE-28 cells (Fig. 5D). The SFRP1-induced senescence phenotype was also observed in primary mammary epithelial cells (Fig. 5E). Interestingly, MCF-7 breast cancer cells, which lack SFRP1 expression due to promoter methylation (38), also displayed a senescence phenotype upon recombinant SFRP1 treatment (Fig. 5F).

Taken together, these results suggest that SFRP1 functions as a secreted mediator of senescence.

Senescence induction by Wnt inhibition. SFRP1 directly binds to the Wnt family proteins and prevents their binding to the Frizzled family receptors, thereby functioning as a secreted inhibitor of Wnt signaling. Downregulation of Wnt signaling was previously shown to occur upon replicative and Ras-induced senescence of human primary fibroblasts, and RNAi knockdown of Wnt2 caused senescence in these cells (44). Therefore, we were interested in whether SFRP1 induces senescence by inhibiting the Wnt signaling.

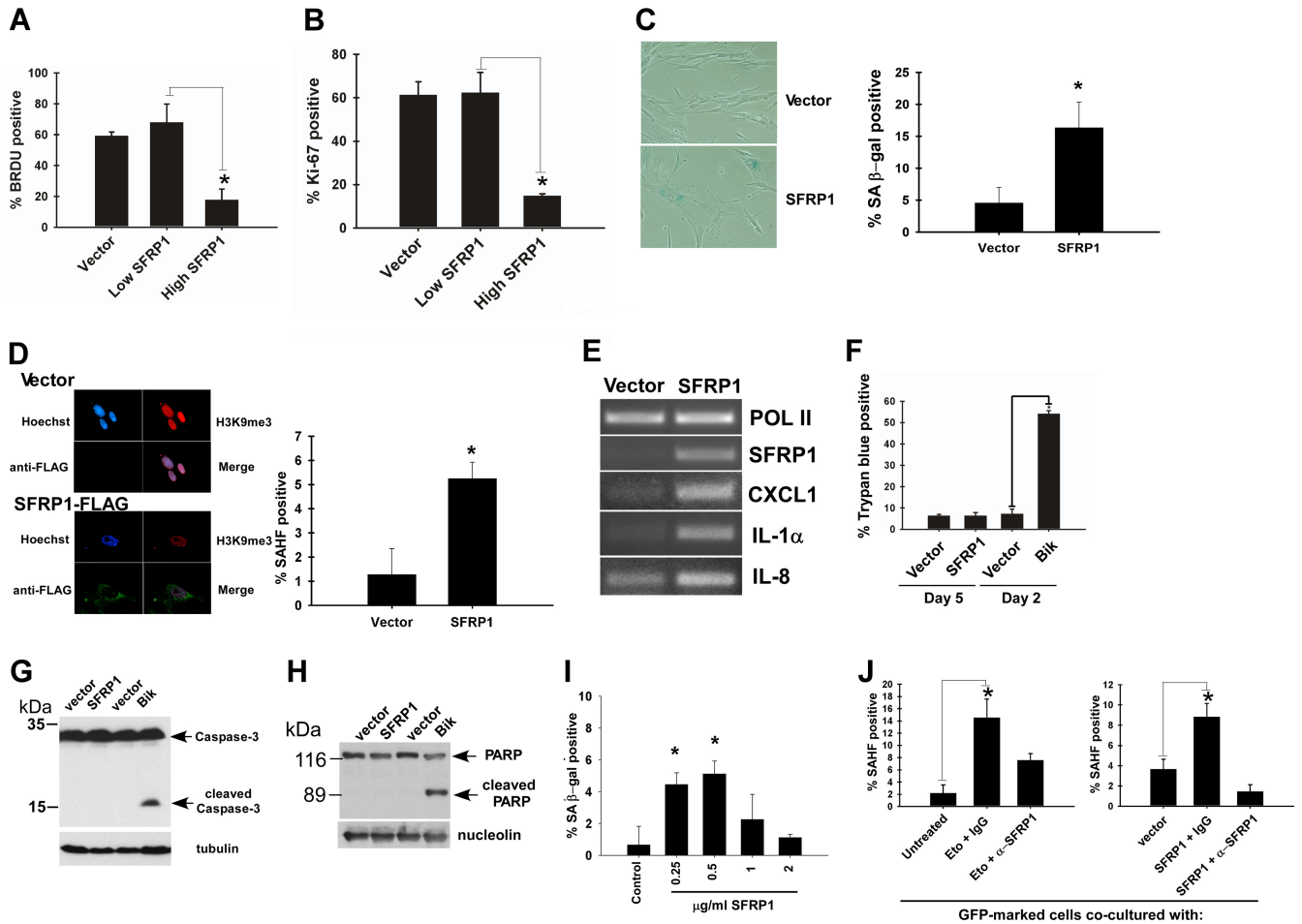Binding of extracellular Wnt to Frizzled receptor results in dis-

FIG 4 SFRP1 induces senescence. (A and B) SFRP1 inhibits cell proliferation. IMR-90 cells were infected with empty lentiviral vector or C-terminally FLAG-tagged SFRP1 lentivirus and were selected with 2 μg/ml puromycin. (A) BrdU incorporation. Four days after infection, the cells were labeled with BrdU for 24 h and stained with antibodies against BrdU and SFRP1. Immunofluorescence microscopy was used to detect the cells displaying no SFRP1 or low SFRP1 expression (Low SFRP1) and those displaying high SFRP1 expression (High SFRP1), and the percentage of BrdU-positive cells was scored. (B) Ki-67 staining. Five days after infection, the cells were stained for Ki-67 and FLAG (SFRP1). *, $P < 0.05$. (C and D) SFRP1 lentivirus induces senescence phenotypes. IMR-90 cells were infected with empty lentiviral vector or SFRP1 lentivirus and were selected with 2 μg/ml puromycin. Five days after infection, the cells were stained for SA-β-Gal (C) or SAHF (D). *, $P < 0.05$ compared to vector control. (E) SFRP1 induces senescence-associated secretory phenotype genes. The expression of CXCL1, IL-1α, and IL-8 was examined by RT-PCR 5 days after SFRP1 viral expression of IMR-90 cells. RNA polymerase II (Pol II) served as a loading control. (F) Trypan blue staining. IMR-90 cells expressing SFRP1 (5 days after infection) or Bik (2 days after infection) were assessed for cell death by dye exclusion assays. (G) Caspase 3 cleavage. IMR-90 cells expressing SFRP1 or Bik were assessed for caspase 3 cleavage by immunoblotting with tubulin as a loading control. (H) PARP cleavage. IMR-90 cells expressing SFRP1 or Bik were assessed for PARP cleavage by immunoblotting with nucleolin as loading control. (I) Recombinant SFRP1 induces senescence in IMR-90 cells. IMR-90 cells were treated with the indicated concentration of recombinant SFRP1 for 4 days and were stained for SA-β-Gal. *, $P < 0.05$ compared to untreated control. (J) Nonsenescent IMR-90 cells acquire a senescence phenotype upon coculture with senescent cells. Nonsenescent IMR-90 cells were infected with GFP-expressing lentivirus. These GFP-labeled IMR-90 cells were cocultured with either senescent IMR-90 cells (induced to senesce by etoposide treatment [left] or by SFRP1 lentiviral expression [right]), or nonsenescent IMR-90 cells (untreated or vector infected) for 4 days. Where indicated, the cells were treated with 1 μg/ml of control IgG or anti-SFRP1 antibody beginning 24 h after initiation of coculture. The GFP-positive cells were scored for the development of senescence-associated heterochromatic foci (SAHF). *, $P < 0.05$. Note that the GFP-positive cells in coculture were not positive for the DNA damage marker γH2AX, indicating that the spreading of senescence is not due to residual etoposide or SFRP1-induced DNA damage.

ruption of a multiprotein complex containing glycogen synthase kinase 3 (GSK3) and its substrate β-catenin, leading to prevention of β-catenin phosphorylation by GSK3 and accumulation of soluble β-catenin, which translocates to the nucleus and activates the transcription of Wnt target genes in conjunction with the T cell factor (TCF) family transcription factors (8, 9). We tested whether SFRP1 can inhibit Wnt signaling in IMR-90 cells. Lentiviral SFRP1 expression in IMR-90 cells resulted in reduced soluble β-catenin (Fig. 6A). Interestingly, etoposide treatment of IMR-90 cells, which stimulates SFRP1 secretion (Fig. 1A), also reduced

soluble β-catenin levels (Fig. 6A). SFRP1 knockdown abolished etoposide-induced reduction of soluble β-catenin levels (Fig. 6B), suggesting that SFRP1 mediates the downregulation of Wnt signaling upon etoposide treatment. Suppression of Wnt signaling by SFRP1 and etoposide treatment was also verified by Wnt-responsive reporter assays: Wnt3 efficiently activated the Super TopFlash reporter in IMR-90 cells, which was almost completely repressed by coexpression of SFRP1 (Fig. 6C). SFRP1 was also able to repress the basal TopFlash reporter activity in IMR-90 cells (data not shown). Furthermore, etoposide treatment repressed
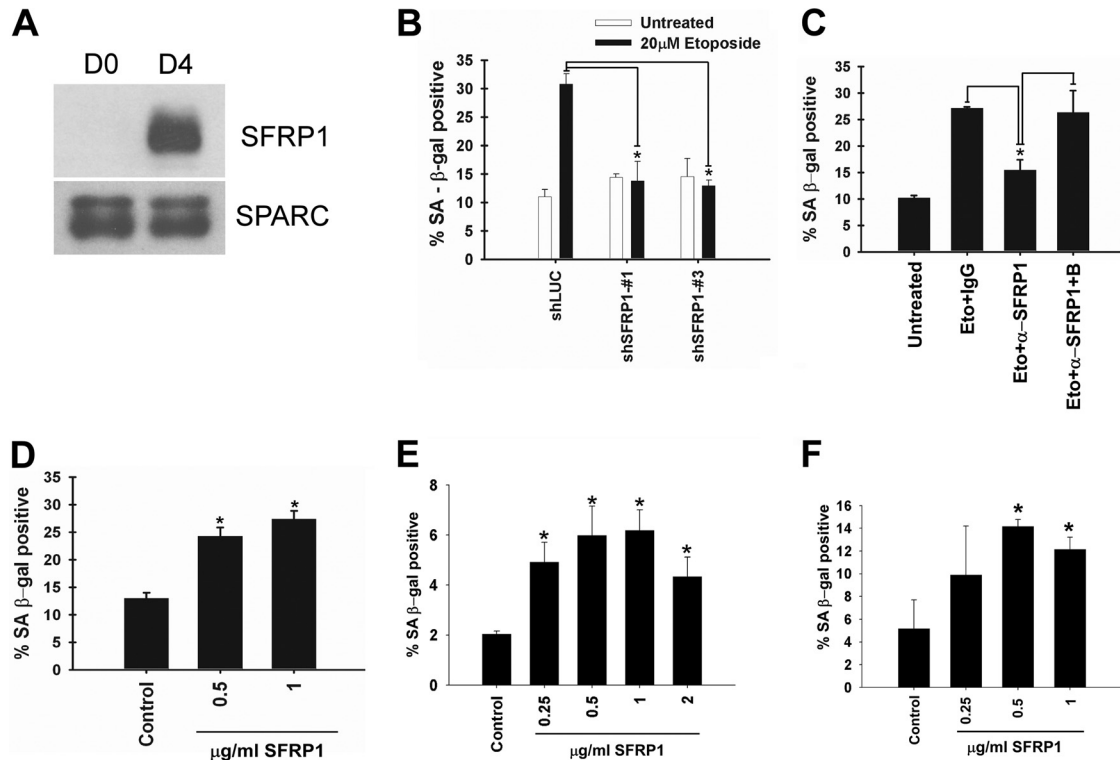
FIG 5 SFRP1 mediates senescence in epithelial cells. (A) Secretion of SFRP1 from etoposide-treated RPE-28 cells. RPE-28 retinal pigment epithelial cells were treated with 20 μM etoposide for 48 h. Four days after the etoposide treatment was initiated, conditioned medium was collected and concentrated. Conditioned medium from untreated cells (D0) was also included as a control. Ten micrograms of each conditioned medium was analyzed for SFRP1 levels by immunoblotting. SPARC served as a loading control. (B) SFRP1 shRNAs attenuates etoposide-induced senescence in RPE-28 cells. RPE-28 cells were infected with lentiviruses expressing shRNA against luciferase or shRNAs against SFRP1 and were selected with 2 μg/ml puromycin. The effect of SFRP1 shRNAs on etoposide-induced senescence of RPE-28 cells was analyzed 6 days after etoposide treatment. *, $P < 0.05$ compared to shLuc plus 20 μM etoposide. (C) SFRP1 antibody inhibits etoposide-induced senescence in RPE-28 cells. RPE-28 cells were treated for 48 h with etoposide. Beginning 24 h after treatment, the cells were incubated with 1 μg/ml of control rabbit IgG, anti-SFRP1 antibody, or anti-SFRP1 antibody plus immunogen (block [B]). Cells were assayed for SA-β-Gal staining at 5 days after etoposide treatment. *, $P < 0.05$ compared to etoposide plus the IgG control or to etoposide plus anti-SFRP1 plus block. (D) Recombinant SFRP1 induces senescence in RPE-28 cells. RPE-28 cells were treated with the indicated concentration of recombinant SFRP1 for 4 days and were stained for SA-β-Gal. *, $P < 0.05$ compared to untreated control. Human primary mammary epithelial cells (E) or MCF-7 breast cancer cells (F) were treated with the indicated concentration of recombinant SFRP1 for 4 days and were stained for SA-β-Gal. *, $P < 0.05$ compared to untreated control.

the basal TopFlash reporter activity in IMR-90 cells, and this repression was abolished by anti-SFRP1 antibody (Fig. 6D). These results suggest that etoposide treatment of IMR-90 cells results in silencing of Wnt signaling through SFRP1.

We then asked whether activation of Wnt signaling can counteract SFRP1-induced and etoposide-induced senescence. As shown in Fig. 6E, coexpression of Wnt3 resulted in significant suppression of SFRP1-induced senescence. The bypass of SFRP1-induced senescence by Wnt3 was accompanied by reactivation of Wnt signaling, as determined by soluble β-catenin levels (Fig. 6F) and Super TopFlash reporter assays (Fig. 6G). SFRP1-induced senescence was also inhibited by lithium chloride treatment, which inhibits GSK3 and activates Wnt/β-catenin signaling (Fig. 6H). Furthermore, etoposide-induced senescence was alleviated by expression of Wnt3 (Fig. 6I). These results suggest that SFRP1 and etoposide induce senescence via inhibition of Wnt signaling. Wnt3 also abrogated hydrogen peroxide-induced senescence of IMR-90 cells (Fig. 6J), suggesting that inhibition of Wnt signaling also mediates oxidative stress-induced senescence.

The role of Wnt inhibition in senescence was further confirmed by pharmacological inhibition of Wnt signaling and shRNA-mediated suppression of β-catenin. Using a *Xenopus* egg

extract screening method, pyrvinium pamoate was recently identified as a potent inhibitor of Wnt signaling (40). We found that treatment of IMR-90 cells with pyrvinium pamoate results in the induction of a senescence phenotype (Fig. 6K). Furthermore, shRNA-mediated silencing of β-catenin (Fig. 6L) caused senescence in IMR-90 cells (Fig. 6M). Interestingly, β-catenin shRNA-2, which almost completely knocked down β-catenin expression, caused a high frequency of SA-β-Gal-positive cells whereas β-catenin shRNA-1, which only partially silenced β-catenin expression, generated fewer SA-β-Gal-positive cells. This suggests that there is a correlation between the extent of Wnt target suppression and senescence induction. Although oncogene-induced senescence was proposed as a consequence of DNA damage (3, 12), phosphorylated histone H2AX staining was not observed upon senescence induced by SFRP1, β-catenin knockdown, or pyrvinium pamoate treatment (data not shown).

SFRP1 belongs to the SFRP family of secreted Wnt antagonists. In humans, there are five SFRP family members, all of which can inhibit Wnt signaling (4, 20). As shown in Fig. 6N, all five SFRP1 family members induced senescence in IMR-90 cells upon lentiviral expression, indicating that senescence induction is a shared property among SFRP family members. In addition to the SFRP
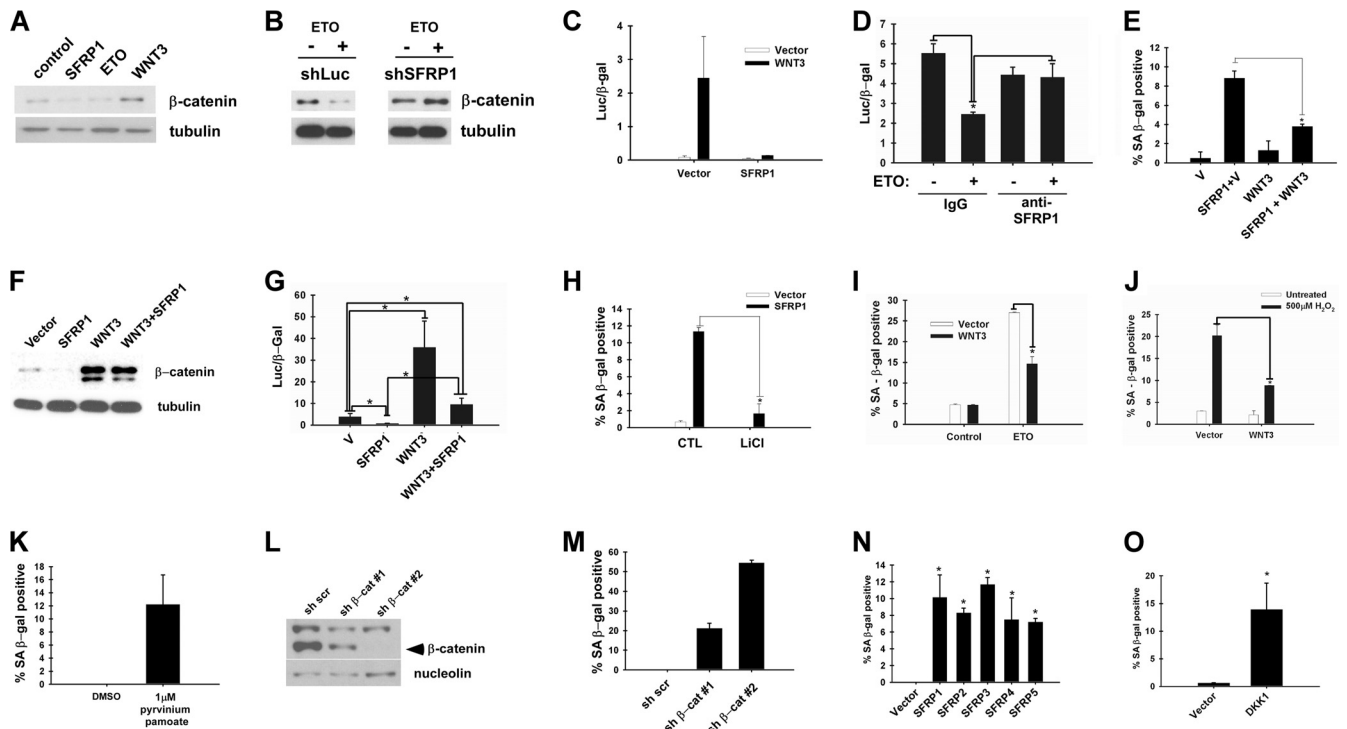
FIG 6 Wnt inhibition results in senescence. (A) SFRP1 reduces soluble β-catenin levels in IMR-90 cells. IMR-90 cells were infected with vector, SFRP1, or Wnt3 lentivirus or treated with 20 μM etoposide. Five days later, soluble β-catenin levels were analyzed by immunoblotting using 5 μg of each soluble fraction. (B) SFRP1 knockdown abrogates etoposide-induced reduction of soluble β-catenin levels. IMR-90 cells were infected with lentiviruses expressing shRNA against luciferase (shLuc) or shRNA against SFRP1 (shSFRP1-3). The cells were treated with 20 μM etoposide, and 5 days later, soluble β-catenin levels were analyzed by immunoblotting using 5 μg of each soluble fraction. (C) SFRP1 silences Wnt-dependent transcription in IMR-90 cells. IMR-90 cells were cotransfected with Super TopFlash reporter, cytomegalovirus (CMV)-β-Gal, and empty vector, SFRP1, or Wnt3 where indicated, and the luciferase activity was determined 48 h after transfection. Transfection efficiencies were normalized using CMV-β-Gal activity. (D) Etoposide treatment represses TopFlash reporter activity. IMR-90 cells were treated with 20 μM etoposide or left untreated for 24 h prior to transfection. The cells were transfected with Super TopFlash reporter and CMV-β-Gal for 4 h, and 1 μg/ml anti-SFRP1 antibody (H-90) or IgG was added after removal of the transfection mixture. The luciferase activity was determined 48 h after transfection. Transfection efficiencies were normalized using CMV-β-Gal activity. *, $P < 0.05$. (E) Wnt3 counteracts SFRP1-induced senescence. IMR-90 cells were infected with the indicated lentiviruses, and 5 days after infection, the cells were stained for SA-β-Gal. *, $P < 0.05$. (F) Wnt3 counteracts SFRP1-induced reduction of soluble β-catenin levels. Soluble β-catenin levels were analyzed by immunoblotting. (G) Wnt3 counteracts SFRP1-induced repression of TopFlash reporter activity. IMR-90 cells were transfected with Super TopFlash reporter and CMV-β-Gal in conjunction with SFRP1 or Wnt3 as indicated. *, $P < 0.05$. (H) LiCl treatment suppresses SFRP1-induced senescence. IMR-90 cells were infected with vector or SFRP1 lentivirus, and 3 days after infection, the cells were treated with 20 mM LiCl for 48 h and stained for SA-β-Gal. *, $P < 0.05$. (I) Wnt3 counteracts etoposide-induced senescence. IMR-90 cells were infected with Wnt3 or empty vector lentivirus. The cells were treated with 20 μM etoposide or left untreated, and the SA-β-Gal activity was analyzed 6 days after etoposide treatment. *, $P < 0.05$. (J) Wnt3 counteracts oxidative stress-induced senescence. IMR-90 cells were treated with 500 μM H$_2$O$_2$ for 2 h. The subsequent day, the cells were infected with lentiviruses expressing Wnt3 or empty vector. On day 6 after H$_2$O$_2$ treatment, the cells were analyzed for SA-β-Gal. *, $P < 0.05$. (K) Pharmacological inhibition of Wnt signaling results in senescence. IMR-90 cells were treated with dimethyl sulfoxide (DMSO) control or 1 μM pyrvinium pamoate for 4 days and were stained for SA-β-Gal. (L) shRNA knockdown of β-catenin. IMR-90 cells were infected with lentiviruses expressing scrambled shRNA (sh scr), shRNA against β-catenin-1 (sh β-cat#1), or shRNA against β-catenin-2 (sh β-cat#2) (sh β-cat 2) and 5 days after infection, β-catenin protein levels were analyzed by immunoblotting. Nucleolin served as a loading control. (M) β-Catenin knockdown results in senescence. IMR-90 cells were infected with the indicated lentiviruses and at 5 days postinfection stained for SA-β-Gal. (N) All five SFRP family members induce senescence. IMR-90 cells were infected with lentiviruses expressing the indicated SFRP family members. At 5 days postinfection, the cells were stained for SA-β-Gal. *, $P < 0.05$ compared to vector control. (O) DKK1 induces senescence. IMR-90 cells were infected with vector or DKK1 lentivirus. At 5 days postinfection, the cells were stained for SA-β-Gal. *, $P < 0.05$ compared to vector control.

family proteins, Wnt signaling is also negatively regulated by another class of secreted antagonists. The DKK family proteins bind to Wnt coreceptors, LRP5/LRP6, and silence Wnt/β-catenin signaling (31). Like SFRP family genes, the DKK family genes are silenced by promoter methylation in different tumor types (31). We found that lentiviral expression of DKK1 also induces senescence in IMR-90 cells (Fig. 6O).

Collectively, these results underscore the role of inhibition of Wnt signaling in cellular senescence.

Role of Rb and p53 pathways in senescence induction by Wnt inhibition. Although the molecular mechanism of cellular senes-

cence is not yet fully understood, the Rb and p53 pathways were shown to play important roles in the establishment of senescence phenotypes (6, 22). Hence, we investigated the status of the Rb and p53 pathways upon SFRP1-induced or β-catenin RNAi-induced senescence as well as the roles of Rb and p53 in the senescence induction.

As shown in Fig. 7A, lentiviral SFRP1 expression in IMR-90 cells resulted in dephosphorylation of Rb, but the expression of p53 and a p53 transcriptional target, p21, remained unchanged, suggesting that SFRP1 activates the Rb pathway, but not the p53 pathway. SFRP1 did not affect the expression of p16 (Fig. 7A, left),
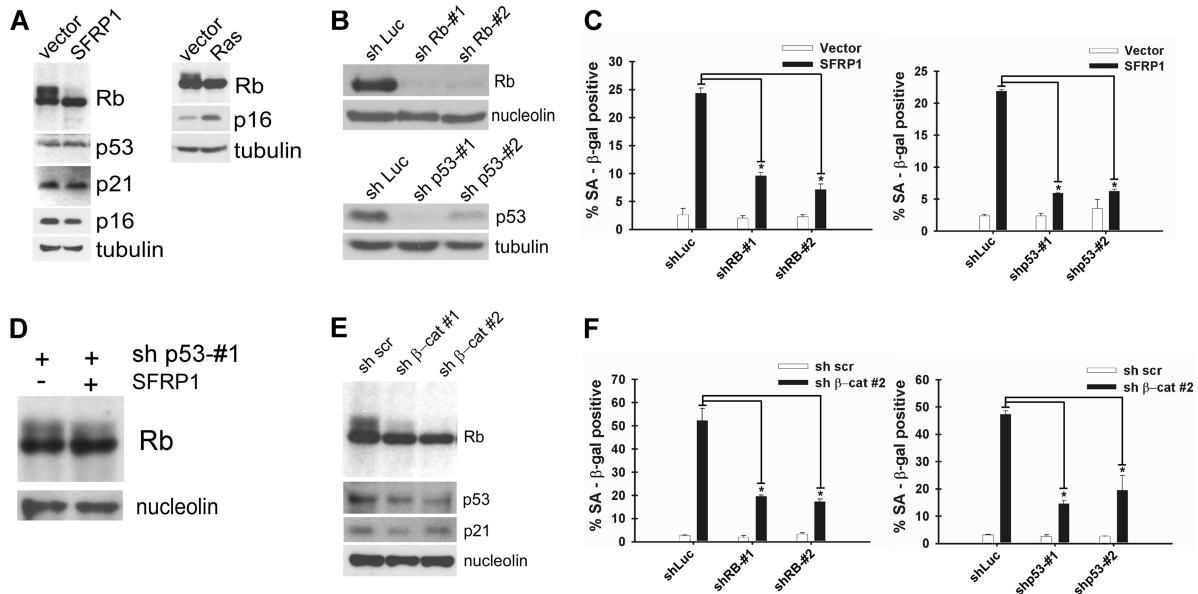
FIG 7 Role of Rb and p53 pathways in senescence induction by Wnt inhibition. (A) Rb dephosphorylation upon SFRP1 expression. IMR-90 cells were infected with vector or SFRP1 lentivirus, and 5 days after infection, Rb, p53, p21, p16, and tubulin expression was analyzed by immunoblotting. SFRP1 induced Rb dephosphorylation but did not affect p53, p21, or p16 expression. For comparison, Rb, p16, and tubulin expression upon Ras-induced senescence was also analyzed by immunoblotting. (B) Knockdown of Rb and p53 in IMR-90 cells. IMR-90 cells were infected with the indicated lentiviruses. Five days after infection, Rb, p53, nucleolin, and tubulin expression was analyzed by immunoblotting. sh, shRNA. (C) Knockdown of Rb or p53 abolishes SFRP1-induced senescence. IMR-90 cells were coinfected with the indicated lentiviruses. Five days postinfection, the cells were stained for SA-β-Gal. *, $P < 0.05$ compared to SFRP1 plus shLuc. (D) p53 knockdown attenuates Rb dephosphorylation by SFRP1. IMR-90 cells were coinfected with the indicated lentiviruses, and 5 days after infection, Rb expression was analyzed by immunoblotting. (E) β-Catenin knockdown results in Rb dephosphorylation. IMR-90 cells were infected with lentiviruses expressing scrambled shRNA (sh scr), shRNA against β-catenin-1 (sh β-cat 1), or shRNA against β-catenin-2 (sh β-cat#2), and 5 days after infection, Rb, p53, and p21 expression was analyzed by immunoblotting. Nucleolin served as a loading control. (F) Knockdown of Rb or p53 abolishes β-catenin RNAi-induced senescence. IMR-90 cells were coinfected with the indicated lentiviruses and 5 days after infection stained for SA-β-Gal. *, $P < 0.05$ compared to sh β-catenin 2 plus shLuc.

a cyclin-dependent kinase inhibitor which plays a key role in the regulation of Rb phosphorylation. In contrast, Rb dephosphorylation as well as p16 induction was observed upon Ras-induced senescence (Fig. 7A, right). We next assessed the role of the Rb and p53 pathways in SFRP1-induced senescence by shRNA-mediated knockdown. Rb and p53 were efficiently silenced by corresponding shRNAs (Fig. 7B), and upon SFRP1 expression, we observed significantly attenuated senescence induction in cells with Rb or p53 knockdown (Fig. 7C). This suggests that in addition to Rb, p53 is required for SFRP1-induced senescence even though SFRP1 does not activate the p53 pathway (Fig. 7A). A possible explanation for this may be derived from the finding that SFRP1-induced Rb dephosphorylation was diminished in cells with p53 knockdown (Fig. 7D).

In parallel, we also examined the contribution of the Rb and p53 pathways to β-catenin RNAi-induced senescence. β-Catenin knockdown resulted in dephosphorylation of Rb but did not induce p53 or p21 (Fig. 7E). β-Catenin RNAi-induced senescence was significantly impaired in cells with Rb or p53 knockdown (Fig. 7F). These results are strikingly similar to the above-mentioned results for SFRP1-induced senescence, which suggests that downregulation of Wnt/β-catenin signaling culminates in the activation of the Rb pathway and induction of senescence.

Cancer-associated SFRP1 mutants are defective for senescence induction. Although the primary mode of SFRP1 inactivation in tumors appears to be transcriptional silencing by promoter methylation (4, 20, 38), there are also reports of cancer-associated

mutations in the coding region of SFRP1 such as a nonsense mutation that prematurely terminates protein translation at codon 151 (N150) in colon cancer (5) and a C140Y point mutation in glioblastoma (the latter mutation was retrieved from the Sanger Institute Catalogue of Somatic Mutations In Cancer web site [http://www.sanger.ac.uk/cosmic]) (2). Both of these mutations affect the N-terminal cysteine-rich domain implicated in Wnt interaction, but their functional consequences have not yet been determined.

We first tested the activity of these two SFRP1 mutants by Super TopFlash reporter assays. As shown in Fig. 8A, whereas wild-type SFRP1 efficiently silenced Wnt3-mediated activation of the Super TopFlash reporter, N150 and C140Y mutants only modestly inhibited Wnt3-induced Super TopFlash activation. Importantly, compared with wild-type SFRP1, these two mutants displayed a considerably impaired ability to induce senescence in IMR-90 cells (Fig. 8B). The expression of SFRP1 N150 was detectable in the brefeldin A-treated cell lysate (Fig. 8C, left) but not in the conditioned medium (Fig. 8C, right), suggesting that this mutant has a defect in secretion or is unstable in the extracellular space. The SFRP1 C140Y mutant displayed expression levels comparable to those of the wild-type SFRP1 both in the brefeldin A-treated lysate and in the conditioned medium (Fig. 8C). Further, these two SFRP1 mutants displayed a compromised ability to induce dephosphorylation of Rb (Fig. 8D). Unlike wild-type SFRP1, the C140Y mutant was unable to inhibit IMR-90 cell proliferation (Fig. 8E to H). These results indicate that the cancer-associated
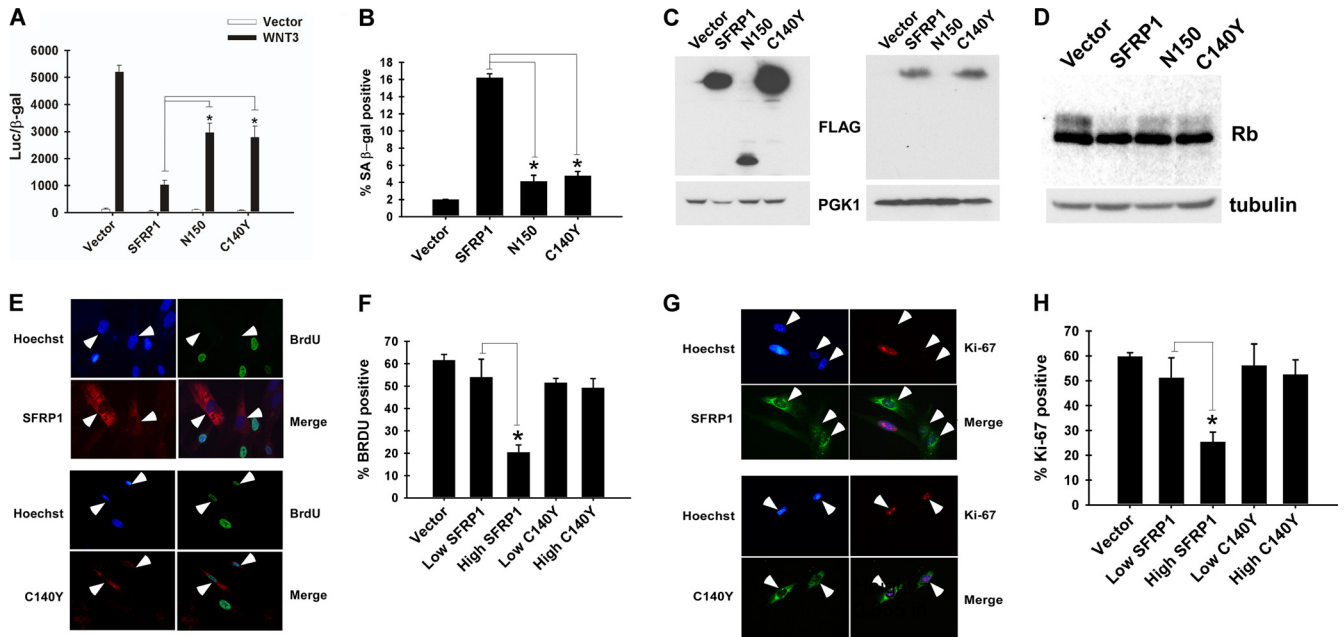
FIG 8 Cancer-associated SFRP1 mutants are defective for senescence induction. (A) Cancer-associated SFRP1 mutants display compromised Wnt-inhibitory activity. 293 cells were cotransfected with Super TopFlash reporter, CMV-β-Gal, and plasmids encoding Wnt3, SFRP1, SFRP1 mutants found in human cancers (N150 or C140Y), or empty vector as indicated. The luciferase activity was determined 48 h after transfection. Transfection efficiencies were normalized using CMV-β-Gal activity. *, $P < 0.05$. (B) Cancer-associated SFRP1 mutants are defective for senescence induction. IMR-90 cells were infected with the indicated lentiviruses and at 5 days postinfection stained for SA-β-Gal. *, $P < 0.05$. (C) Expression levels of wild-type and mutant SFRP1. IMR-90 cells were infected with lentiviruses encoding SFRP1 or the N150 or C140Y mutant (all C-terminally FLAG tagged). Five days postinfection, the expression levels of wild-type and mutant SFRP1 were analyzed by anti-FLAG immunoblotting of the brefeldin A-treated cell lysate (left) and the conditioned medium (right). (D) SFRP1 mutants display impaired ability to induce dephosphorylation of Rb. IMR-90 cells were infected with vector lentivirus or lentivirus encoding SFRP1, N150, or C140Y, and 5 days after infection, Rb expression was analyzed by immunoblotting. Tubulin served as a loading control. (E to H) The SFRP1 C140Y mutant is unable to inhibit cell proliferation. IMR-90 cells were infected with empty lentiviral vector or lentiviruses expressing wild-type or C140Y mutant SFRP1. Cell proliferation was assessed by BrdU incorporation (E and F) and by Ki-67 staining (G and H) as described in the legend of Fig. 4A and B. The cells expressing wild-type or C140Y SFRP1 are indicated by arrowheads in panels E and G. *, $P < 0.05$.

SFRP1 mutants are defective for antagonizing Wnt signaling and inducing senescence.

DISCUSSION

Given the frequent SFRP1 gene silencing in a wide variety of tumor types as well as SFRP1-mediated inhibition of tumor cell proliferation, SFRP1 has long been considered a tumor suppressor, but its biological function(s) relevant to tumor suppression remained poorly defined. This study revealed a novel senescence-inducing activity of SFRP1 and raised a possibility that SFRP1 suppresses tumors by acting as a secreted mediator of cellular senescence.

We have found that different stresses such as DNA or oxidative damage induce SFRP1 secretion from human primary fibroblasts (Fig. 1A and J) and that secreted SFRP1 in turn mediates senescence phenotypes in stressed fibroblasts (Fig. 3B to D and F). Lentiviral expression of SFRP1 caused proliferation arrest and senescence phenotypes in primary fibroblasts (Fig. 4A to E). Furthermore, addition of purified recombinant SFRP1 to the culture medium induced senescence in primary fibroblasts (Fig. 4I), which suggests that extracellular SFRP1 can directly induce senescence. SFRP1 also mediated senescence in epithelial cells. Upon etoposide treatment, retinal pigment epithelial cells oversecreted SFRP1 (Fig. 5A), and SFRP1 shRNAs or anti-SFRP1 antibody treatment attenuated etoposide-induced senescence in these cells (Fig. 5B and C). Further, recombinant SFRP1 induced a senes-

cence phenotype in retinal pigment epithelial cells (Fig. 5D), mammary epithelial cells (Fig. 5E), and MCF-7 breast cancer cells (Fig. 5F). MCF-7 cells are one of many cancer cell lines whose SFRP1 loci are silenced by promoter methylation (38), and senescence induction by reexposing MCF-7 to SFRP1 is consistent with the notion that the evasion of SFRP1-induced senescence contributes to tumorigenesis. Lending further support to this notion is the finding that the senescence-inducing activity of SFRP1 is impaired in SFRP1 mutants found in glioblastoma and colon cancer (Fig. 8B). Inactivation of SFRP1 by promoter methylation or by mutation of the coding region may allow preneoplastic cells to escape stress-induced senescence and accumulate further mutations to develop into a full-blown tumor. We note, however, that SFRP1 is reported to sensitize cells to apoptosis (27), which might also contribute to tumor suppression.

We also provided several lines of evidence suggesting that SFRP1 induces senescence by antagonizing Wnt signaling. SFRP1 expression in IMR-90 fibroblasts, which induced senescence phenotypes, also resulted in reduced soluble β-catenin levels (Fig. 6A) and repression of Wnt/β-catenin-dependent transcription (Fig. 6C). SFRP1-induced senescence was inhibited by coexpression of Wnt3 (Fig. 6E) or by lithium chloride-mediated stimulation of Wnt signaling (Fig. 6H). Furthermore, cancer-associated SFRP1 mutants that display compromised senescence-inducing activity were also defective for antagonizing Wnt signaling (Fig. 8A). We also demonstrated senescence-inducing activity for all five SFRP

family members (Fig. 6N) as well as DKK1 (Fig. 6O), which belongs to a distinct class of secreted Wnt antagonists. The role of Wnt inhibition in cellular senescence was also supported by senescence induction upon pharmacological inhibition of Wnt signaling (Fig. 6K) and upon knockdown of β-catenin (Fig. 6M). Previous work by Ye et al. indicated that Wnt2 expression and Wnt signaling are repressed in human fibroblasts undergoing replicative senescence or Ras-induced senescence and that Wnt2 RNAi induces senescence phenotypes in human fibroblasts (44). Our study extended these observations by revealing the role of secreted Wnt antagonists in senescence induction and further established the link between Wnt downregulation and cellular senescence.

In terms of the downstream target of SFRP1, we demonstrated that SFRP1-induced senescence is accompanied by dephosphorylation of Rb (Fig. 7A) and that Rb knockdown abolishes SFRP1-induced senescence (Fig. 7C), indicating the critical importance of the Rb pathway in SFRP1-induced senescence. p53 knockdown also abolished SFRP1-induced senescence (Fig. 7C); however, we believe this is secondary to the compromised Rb dephosphorylation by SFRP1 in p53 knockdown cells (Fig. 7D) since SFRP1 expression in primary fibroblasts did not induce p53 or a p53 transcriptional target, p21 (Fig. 7A). β-Catenin RNAi-induced senescence was also accompanied by Rb dephosphorylation (Fig. 7E), and Rb knockdown abolished β-catenin RNAi-induced senescence (Fig. 7F), further supporting the role of the Rb pathway in Wnt downregulation-induced senescence.

One possible mechanism for Rb activation by Wnt downregulation is through repression of Wnt/β-catenin target genes such as CDC25A, c-Myc, and cyclin D, which play critical roles in the G_1/S transition and regulate Rb phosphorylation. However, we did not observe significant changes in the expression of these Wnt target genes upon SFRP1-induced senescence (data not shown). Alternatively, a nontranscriptional function(s) of Wnt/β-catenin pathway may modulate Rb phosphorylation and senescence induction. Recent work demonstrated that Wnt signaling inactivates GSK3 by sequestering the enzyme in multivesicular bodies (MVBs), which affects the half-life of 20% of all cellular proteins (39). Interestingly, β-catenin also localizes in MVBs and is required for MVB formation (39). Altered half-lives of critical signaling proteins upon Wnt downregulation might contribute to Rb dephosphorylation and senescence induction.

While a large body of evidence supports the role of SFRP1 and other SFRP family members as human tumor suppressors, inactivation of SFRP family members in mice, thus far, has not been shown to result in tumorigenesis. SFRP1 knockout mice displayed abnormal bone formation but did not develop tumors up to 2 years of age (41). We tested the effect of SFRP1 expression in mouse embryonic fibroblasts and did not observe proliferation arrest or senescence phenotypes. There are a number of important differences between human and mouse cells including a critical difference in sensitivity to oxidative stress (33). In fact, mouse embryonic fibroblasts were reported to undergo senescence upon Wnt signaling due to increased mitochondrial biogenesis and concomitant generation of reactive oxygen species (45). Although the lack of tumors in SFRP knockout mice could be due to compensation by remaining SFRP family members, it is also possible that there are species differences in senescence induction and tumor suppression by SFRPs.

Wnt signaling is deregulated in a large number of human tumor types, and together with Notch signaling, it was classified as one of 12 commonly altered, core signaling pathways in human pancreatic cancers (19). Recently, several chemical inhibitors of Wnt signaling were developed and were reported to display antitumor activity (7, 18, 40). A chemical screen for compounds that both stabilize Axin and promote β-catenin turnover identified an FDA-approved drug, pyrvinium pamoate, as a potent inhibitor of Wnt signaling (40). Pyrvinium selectively activates casein kinase 1α, which results in stabilization of Axin and degradation of β-catenin and Pygopus, a nuclear cofactor of β-catenin. Pyrvinium treatment of colon cancer cells with deregulated Wnt signaling efficiently inhibited proliferation (40). Consistent with a link between Wnt downregulation and cellular senescence, we found that pyrvinium displays senescence-inducing activity (Fig. 6K). Compounds that mimic or enhance the action of SFRP1 and other secreted Wnt antagonists may become a new class of anticancer agents that suppress cancer proliferation by inducing senescence.

Based on the results presented here, we propose that SFRP1 is an extracellular component of stress-induced senescence signaling that responds to potentially carcinogenic stresses such as DNA damage and oxidative insult and induces cellular senescence in an autocrine and paracrine fashion, which may lead to non-cell-autonomous tumor suppression. As noted above, the other four SFRP family members as well as DKK1 are also able to induce senescence although the stimuli that induce the secretion of these Wnt antagonists are not well understood. Future work should clarify the precise roles of secreted Wnt antagonists in cellular senescence and tumor suppression.

ACKNOWLEDGMENTS

REFERENCES

1. **Acosta JC, et al.** 2008. Chemokine signaling via the CXCR2 receptor reinforces senescence. Cell **133**:1006–1018.
2. **Bamford S, et al.** 2004. The COSMIC (catalogue of somatic mutations in cancer) database and website. Br. J. Cancer. **91**:355–358.
3. **Bartkova J, et al.** 2006. Oncogene-induced senescence is part of the tumorigenesis barrier imposed by DNA damage checkpoints. Nature **444**:633–637.
4. **Bovolenta P, Esteve P, Ruiz JM, Cisneros E, Lopez-Rios J.** 2008. Beyond Wnt inhibition: new functions of secreted Frizzled-related proteins in development and disease. J. Cell Sci. **121**:737–746.
5. **Caldwell GM, et al.** 2004. The Wnt antagonist sFRP1 in colorectal tumorigenesis. Cancer Res. **64**:883–888.
6. **Campisi J, d'Adda di Fagagna F.** 2007. Cellular senescence: when bad things happen to good cells. Nat. Rev. Mol. Cell Biol. **8**:729–740.
7. **Chen B, et al.** 2009. Small molecule-mediated disruption of Wnt-dependent signaling in tissue regeneration and cancer. Nat. Chem. Biol. **5**:100–107.
8. **Chien AJ, Conrad WH, Moon RT.** 2009. A Wnt survival guide: from flies to human disease. J. Invest. Dermatol. **129**:1614–1627.
9. **Clevers H.** 2006. Wnt/beta-catenin signaling in development and disease. Cell **127**:469–480.
10. **Coppe JP, Desprez PY, Krtolica A, Campisi J.** 2010. The senescence-associated secretory phenotype: the dark side of tumor suppression. Annu. Rev. Pathol. **5**:99–118.
11. **Coppe JP, et al.** 2008. Senescence-associated secretory phenotypes reveal cell-nonautonomous functions of oncogenic RAS and the p53 tumor suppressor. PLoS Biol. **6**:2853–2868.

12. **Di Micco R, et al.** 2006. Oncogene-induced senescence is a DNA damage response triggered by DNA hyper-replication. Nature **444**:638–642.

13. **Dimri GP, et al.** 1995. A biomarker that identifies senescent human cells in culture and in aging skin in vivo. Proc. Natl. Acad. Sci. U. S. A. **92**:9363–9367.

14. **Eng JK, McCormack AL, Yates JR III.** 1994. An approach to correlate tandem mass spectral data of peptides with amino acid sequences in a protein database. J. Am. Soc. Mass Spectrom. **5**:976–989.

15. **Finch PW, et al.** 1997. Purification and molecular cloning of a secreted, Frizzled-related antagonist of Wnt action. Proc. Natl. Acad. Sci. U. S. A. **94**:6770–6775.

16. **Gygi SP, et al.** 1999. Quantitative analysis of complex protein mixtures using isotope-coded affinity tags. Nat. Biotechnol. **17**:994–999.

17. **Hayflick L, Moorhead PS.** 1961. The serial cultivation of human diploid cell strains. Exp. Cell Res. **25**:585–621.

18. **Huang SM, et al.** 2009. Tankyrase inhibition stabilizes axin and antagonizes Wnt signalling. Nature **461**:614–620.

19. **Jones S, et al.** 2008. Core signaling pathways in human pancreatic cancers revealed by global genomic analyses. Science **321**:1801–1806.

20. **Kawano Y, Kypta R.** 2003. Secreted antagonists of the Wnt signalling pathway. J. Cell Sci. **116**:2627–2634.

21. **Keller A, Nesvizhskii AI, Kolker E, Aebersold R.** 2002. Empirical statistical model to estimate the accuracy of peptide identifications made by MS/MS and database search. Anal. Chem. **74**:5383–5392.

22. **Kuilman T, Michaloglou C, Mooi WJ, Peeper DS.** 2010. The essence of senescence. Genes Dev. **24**:2463–2479.

23. **Kuilman T, et al.** 2008. Oncogene-induced senescence relayed by an interleukin-dependent inflammatory network. Cell **133**:1019–1031.

24. **Kuilman T, Peeper DS.** 2009. Senescence-messaging secretome: SMS-ing cellular stress. Nat. Rev. Cancer **9**:81–94.

25. **Lai Y, Qiao M, Song M, Weintraub ST, Shiio Y.** 2011. Quantitative proteomics identifies the Myb-Binding Protein p160 as a novel target of the von Hippel-Lindau tumor suppressor. PLoS One **6**:e16975. doi:10.1371/journal.pone.0016975.

26. **Li XJ, Zhang H, Ranish JA, Aebersold R.** 2003. Automated statistical analysis of protein abundance ratios from data generated by stable-isotope dilution and tandem mass spectrometry. Anal. Chem. **75**:6648–6657.

27. **Melkonyan HS, et al.** 1997. SARPs: a family of secreted apoptosis-related proteins. Proc. Natl. Acad. Sci. U. S. A. **94**:13636–13641.

28. **Narita M, et al.** 2003. Rb-mediated heterochromatin formation and silencing of E2F target genes during cellular senescence. Cell **113**:703–716.

29. **Narita M, et al.** 2011. Spatial coupling of mTOR and autophagy augments secretory phenotypes. Science **332**:966–970.

30. **Nesvizhskii AI, Keller A, Kolker E, Aebersold R.** 2003. A statistical model for identifying proteins by tandem mass spectrometry. Anal. Chem. **75**:4646–4658.

31. **Niehrs C.** 2006. Function and biological roles of the Dickkopf family of Wnt modulators. Oncogene **25**:7469–7481.

32. **Orjalo AV, Bhaumik D, Gengler BK, Scott GK, Campisi J.** 2009. Cell surface-bound IL-1α is an upstream regulator of the senescence-associated IL-6/IL-8 cytokine network. Proc. Natl. Acad. Sci. U. S. A. **106**:17031–17036.

33. **Parrinello S, et al.** 2003. Oxygen sensitivity severely limits the replicative lifespan of murine fibroblasts. Nat. Cell Biol. **5**:741–747.

34. **Rodier F, et al.** 2009. Persistent DNA damage signalling triggers senescence-associated inflammatory cytokine secretion. Nat. Cell Biol. **11**:973–979.

35. **Shiio Y, Aebersold R.** 2006. Quantitative proteome analysis using isotope-coded affinity tags and mass spectrometry. Nat. Protoc. **1**:139–145.

36. **Shiio Y, et al.** 2002. Quantitative proteomic analysis of Myc oncoprotein function. EMBO J. **21**:5088–5096.

37. **Shiio Y, et al.** 2006. Quantitative proteomic analysis of Myc-induced apoptosis: a direct role for Myc induction of the mitochondrial chloride ion channel, mtCLIC/CLIC4. J. Biol. Chem. **281**:2750–2756.

38. **Suzuki H, et al.** 2002. A genomic screen for genes upregulated by demethylation and histone deacetylase inhibition in human colorectal cancer. Nat. Genet. **31**:141–149.

39. **Taelman VF, et al.** 2010. Wnt signaling requires sequestration of glycogen synthase kinase 3 inside multivesicular endosomes. Cell **143**:1136–1148.

40. **Thorne CA, et al.** 2010. Small-molecule inhibition of Wnt signaling through activation of casein kinase 1α. Nat. Chem. Biol. **6**:829–836.

41. **Trevant B, et al.** 2008. Expression of secreted frizzled related protein 1, a Wnt antagonist, in brain, kidney, and skeleton is dispensable for normal embryonic development. J. Cell. Physiol. **217**:113–126.

42. **van Hengel J, et al.** 1997. Protein kinase C activation upregulates intercellular adhesion of alpha-catenin-negative human colon cancer cell variants via induction of desmosomes. J. Cell Biol. **137**:1103–1116.

43. **Veeman MT, Slusarski DC, Kaykas A, Louie SH, Moon RT.** 2003. Zebrafish prickle, a modulator of noncanonical Wnt/Fz signaling, regulates gastrulation movements. Curr. Biol. **13**:680–685.

44. **Ye X, et al.** 2007. Downregulation of Wnt signaling is a trigger for formation of facultative heterochromatin and onset of cell senescence in primary human cells. Mol. Cell **27**:183–196.

45. **Yoon JC, et al.** 2010. Wnt signaling regulates mitochondrial physiology and insulin sensitivity. Genes Dev. **24**:1507–1518.